

Causal Analysis at Extreme Quantiles with Application to London Traffic Flow Data

Kaushik Jana^{1§}, Prajamitra Bhuyan^{1§,†}, Emma J. McCoy^{*,†}

[§] School of Arts and Sciences, Ahmedabad University, India

[§]School of Mathematical Sciences, Queen Mary University of London, United Kingdom

^{*}Department of Mathematics, Imperial College London, United Kingdom

[†]The Alan Turing Institute, United Kingdom

Abstract

Transport engineers employ various interventions to enhance traffic-network performance. Recent emphasises on cycling as a sustainable travel mode aims to reduce traffic congestion. Quantifying the impacts of Cycle Superhighways is complicated due to the non-random assignment of such intervention over the transport network and heavy-tailed distribution of traffic flow. Treatment effects on asymmetric and heavy tailed distributions are better reflected at extreme tails rather than at averages or intermediate quantiles. In such situations, standard methods for estimating quantile treatment effects at the extremes can provide misleading inference due to the high variability of estimates. In this work, we propose a novel method which incorporates a heavy tailed component in the outcome distribution to estimate the extreme tails and simultaneously employs quantile regression to model the bulk part of the distribution utilising a state-of-the-art technique. Simulation results show the superiority of the proposed method over existing estimators for quantile causal effects at extremes in the case of heavy tailed distributions. The analysis of London transport data utilising the proposed method indicates that the traffic flow increased substantially after the Cycle Superhighway came into operation. The findings can assist government agencies in effective decision making to avoid high consequence events and improve network performance.

Key words: Causality, Extreme value analysis, Heavy tailed distribution, Potential outcome, Quantile regression, Transport engineering

¹The authors contribute equally to this paper.

1 Introduction

In the last couple of decades, metropolitan areas in both developed and developing countries, have been affected by increasing traffic congestion due to population explosion. Urban population in developing nations is projected to continue to grow, adding 2.5 billion people to the world's cities by 2050 ([UN Environment Programme, 2019](#)). In addition to the negative impacts on mobility and air quality, previous studies indicate that severe congestion has a negative impact on GDP, the city's economic competitiveness ([Slawson, 2017](#); [Jin and Rafferty, 2017](#)), and road safety, thus imparting socio-economic distress ([Retallack and Ostendorf, 2019](#)). Intelligent transportation systems can revolutionize traffic-mobility management and offers an integrated approach to infrastructure development ([Xian et al., 2021](#)). World-wide transport engineers employ network interventions (i.e. treatment) as measure to control high-consequence events. But, such decisions are made without any statistical evidence to guarantee the intended outcomes. Often such interventions fail to achieve the intended objective and in which transport networks perform poorly in relation to traffic flow, capacity utilisation, safety, and economic and environmental impacts. In general, the intervention are typically targeted to address specific network problems, and its effect is 'confounded' if the treated and control units differ systematically with respect to several characteristics which may affect the outcome of interest.

In the last decade, cycling has been promoted as an affordable, clean and environmentally fit sustainable means of transportation all over the world. The bicycle contributes to cleaner air and less congestion that promotes economic growth and reduces inequalities while bolstering the fight against climate change to achieve sustainable development goals ([United Nations, 2021](#)). A recent study on Traffic Scorecard released in 2021 ranks London as the world's most congested city out of more than 1,000 global cities ([Reid, 2021](#)). The Mayor of London aim for cycling journeys in London to increase from 2% of all journeys in 2001 to 5% by 2026. To promote cycling activity, several policy decisions including the Cycle Superhighways (CS), Santander Cycles and Biking Boroughs have already been implemented ([Transport for London, 2010](#)). The CS are 1.5-meter wide barrier-free cycling paths connecting outer London to central London to provide adequate spatial capacity for existing cyclists and potential future commuters who adopt cycling as a mode of transport (See [Figure 1](#)). Twelve Cycle Superhighways were announced in 2008 with the aim of enabling faster and safer cycle journeys. As displayed in [Figure 2](#), these routes were designed in a clock faced layout to radiate from the city center towards greater London. Currently, only

four routes are in operation, namely CS2 (Stratford to Aldgate); CS3 (Barking to Tower Gateway); CS7 (Merton to the City); and CS8 (Wandsworth to Westminster). In the very first year, cycling has increased by 83% along CS3 and 46% along CS7 after their inauguration in 2010. The effects of CS on heavy congestion are not evaluated in the report by [Transport for London \(2011\)](#) due to lack of adequate data and methodological framework for analysis. However, there are some contradictory reports about the effects of CS on road traffic congestion has been published in print and electronic media ([Norman, 2017](#); [Blunden, 2016](#)). Due to the intricate nature of the transport network, the quantification of the effects of CS on high consequence events like extreme traffic congestion is a complex problem. Moreover, various traffic and socioeconomic characteristics may act as confounders, affecting both the traffic flow and intervention simultaneously, therefore it is important to study the causal association of those factors with the interventions and outcome of interest. For example, business centres with high employment density with interactively connecting roads are expected to have more congestion compared to the residential areas.



Figure 1: Examples of London Cycling Superhighways

The need to develop statistical methods to study causal quantities is important due to their wide application and impact in various fields of science, e.g., medical science ([Imbens and Rubin, 2015](#)), transport engineering ([Li et al., 2017](#); [Zhang et al., 2021](#)), and public policy ([Gangl, 2010](#); [Freedman, 2010](#)). Most commonly, the literature on causal inference is focused on population means

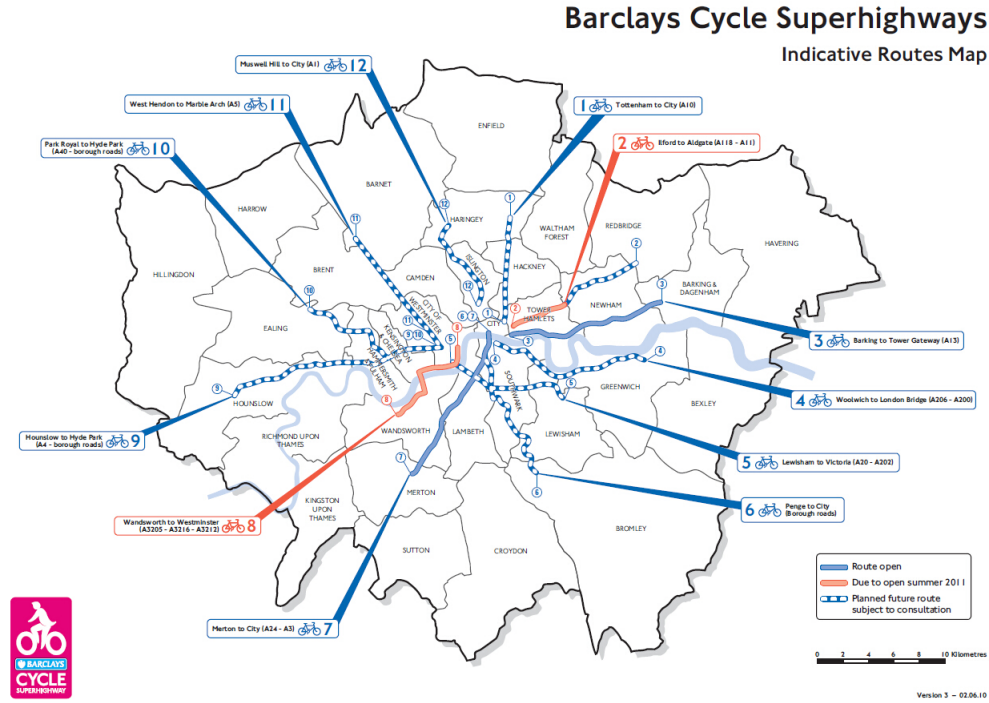


Figure 2: Route map of London Cycling Superhighways

of potential outcomes. In real scenarios, asymmetric and heavy tailed distributions are frequently encountered and treatment effects are often better summarized in tail quantiles rather than in averages. There is a growing literature that focuses directly on the estimation of casual effects on quantiles. [Firpo \(2007\)](#) proposed estimating the quantiles by minimizing an inverse probability weighted check loss function, their estimator achieves non-parametric consistency by means of a propensity score estimated as a logistic power series whose degree increases with sample size. [Melly \(2006\)](#), [Frölich and Melly \(2013\)](#), and [Chernozhukov et al. \(2013\)](#) considered estimation of the quantiles under a linear parametric model for the distribution, and quantile functions, respectively. [Zhang et al. \(2012\)](#) proposed several methods for estimation of causal effects on quantiles which are analogous to the methods employed for the average causal effect. [Díaz \(2017\)](#) proposed a doubly robust estimator based on a semiparametric approach using a targeted maximum likelihood estimator for the quantiles. In this context, [Xu et al. \(2018\)](#) proposed a Bayesian nonparametric approach considering Bayesian additive regression trees to model the propensity score and a Dirichlet process mixture of normal models to construct the distribution of potential outcomes.

Estimation of extreme quantiles (or equivalently, so-called return levels) of univariate and con-

ditional distributions is an important problem in various applications, for example, in meteorology, hydrology, climatology and finance. Extreme value theory provides tools to predict extreme events based on the assumption that the underlying distribution of the normalized random variable resides in the domain of attraction of an extreme value distribution (Fisher and Tippett, 1928). Thus extreme quantiles can be predicted by estimating the parameters of the specific extreme value distribution and the normalizing constants. Detailed reviews on different models and methods of estimation in this context can be found in, for example, Embrechts et al. (1997), and Coles (2001). Zhang (2018) considered the estimator proposed by Firpo (2007) and developed asymptotic theory for the causal estimator at intermediate and extreme quantiles. There is very little work in the literature relating causality and the occurrence of extreme events. Recently Gnecco et al. (2019) and Engelke (2020) proposed causal inference combined with extreme value theory to characterise causal tail dependence of two random variables in the context of a directed acyclic graphical model. Gissibl and Klüppelberg (2018); Gissibl et al. (2017) study the inferential question on the causal dependence structure on acyclic graphs. In their work, Mhalla et al. (2019) studied the causal relationship between two extreme random variables for modelling daily measurements of river discharges corresponding to riverflow-connected stations. This modelling approach uses a copula structure to estimate the dependence between two random variables with the restriction that there are no confounders (common set of covariates affecting treatment and response simultaneously) in the model. Recently, there has been a focus on studying the causal links between external forcing of the climate system and climate change (attribution) and this causal link has been used to design event attribution, see Hannart and Naveau (2018) and Ribes et al. (2020) for further details. For a comprehensive overview of the literature see the review article Naveau et al. (2020).

1.1 London Transport-network Data

We are interested in estimation of the causal effect of London Cycling Superhighways on extreme traffic congestion based on a data set collected over the period 2007-2014. In this study, 75 treated zones and 375 control zones were considered along the 40 km long main corridors radiating from central London to outer London. In observational data, the effect of CS is confounded due to various factors related to traffic dynamics, road characteristics, and socio-demographic conditions. Traffic data on both the major and minor road network are routinely collected by the UK Government's Department for Transport. Also, additional information on traffic flow and speed are collected from the London Atmospheric Emissions Inventory (LAEI). It is observed that traffic congestion is asso-

ciated with bus-stop density and road network density. An association between traffic congestion and socio-demographic characteristics, such as employment and land-use patterns, has also been indicated in previous studies (Badoe and Miller, 2000; Zhang et al., 2017; Chen et al., 2001). See Li et al. (2017) for the detailed data description. To incorporate these effects, we obtained relevant data on population and employment density, as well as the information of land-use patterns from the Office for National Statistics. The data that are available from the aforementioned sources and the rationale to construct the response and covariates are described in Section 5.

Transport engineers have recently emphasized the importance of developing inferential tools that allow us to predict the extreme consequences of interventions or shocks to the system and that enable us to choose the most appropriate interventions to mitigate the consequences of such events (Zheng and Sayed, 2019; Xu and Nusholtz, 2017; FarahaCarlos and Azevedo, 2017). The data set we consider arises from a study of various interventions targeted at traffic conditions in the city of London. An important question for policy makers is to quantify the causal effect of these interventions on the extreme consequences of traffic flow. The outcome we consider exhibits heavy tails as there are a small, but non trivial number of locations with very high traffic flow. Heavy tailed distributions are often characterized by large variances, and the variance of standard estimators of the causal quantities is also very large and subsequently precludes statistical significance at most plausible sample sizes (Díaz, 2017). In this work, we address this issue and propose a method of estimation of the causal effect at the extreme tails by combining tools of causal inference and extreme value theory. We demonstrate the performance of the proposed method through a simulation study and apply our method to the transport engineering application outlined above.

The outline of the article is as follows, in Section 2 we describe the existing models and methods used in the traditional potential outcome framework. In Section 3, we propose a new method to estimate the causal effects at extreme quantiles. Simulation studies are performed to assess the effectiveness of the proposed methods and the results are summarized in Section 4. In Section 5, the results of applying the method on motivating data from London Cycle Superhighways are discussed. We summarise the key findings and conclude with a discussion of future research in Section 6.

2 Potential Outcome Framework

In usual causal inference problems, the data available for estimation of the causal effects are realisations of a random vector, $Z_i = (Y_i, D_i, \mathbf{X}_i)$, $i = 1, \dots, n$, where for the i th unit of observation, Y_i denotes the response, D_i the treatment (intervention or exposure) received, and \mathbf{X}_i a vector of confounders or covariates. The treatment can be binary, multi-valued or continuous but essentially it is not assigned randomly. Therefore, the simple comparisons of average responses across different treatment groups will not in general reveal a ‘causal’ effect (causation) due to potential confounding. Confounding can be addressed if the vector of covariates \mathbf{X}_i is sufficient to ensure unconfoundedness, or conditional independence of potential responses and treatment assignment. In the context of binary treatments, the conditional independence assumption requires that $(Y_i(0), Y_i(1)) \perp\!\!\!\perp \mathbb{I}(D_i) | \mathbf{X}_i$, where $\mathbb{I}(D_i)$ is the indicator function for receiving the treatment and $Y_i(1)$ and $Y_i(0)$ indicate potential outcomes under treated or control status, respectively. An additional requirement for valid causal inference is that, conditional on covariates \mathbf{X}_i , the probability of assignment to treatment is strictly positive for every combination of values of the covariates, i.e. $0 < P[\mathbb{I}(D_i) = 1 | \mathbf{X}_i = \mathbf{x}] < 1$ for all \mathbf{x} . See [Rosenbaum and Rubin \(1983\)](#) for more details. Conventionally, the main interest is in estimating the average treatment effect $\mu = \mathbb{E}[Y_i(1)] - \mathbb{E}[Y_i(0)]$, which measures the difference in average expected outcomes under treatment and control status.

In practice, asymmetric distributions for the response variable are frequently encountered and often summarized using quantiles. If the outcome of interest follows a skewed distribution, the median may be a more appropriate measure of location than the mean, and a statistic based on quantiles may be a more meaningful measure of spread than the standard deviation. In many applications, practitioners are interested in the tail distributions (say higher than 95th percentiles) of the potential outcomes ([Zhang et al., 2012](#); [Díaz, 2017](#)). In the presence of confounding, a simple comparison of the treated and untreated individuals in terms of empirical quantiles would not have a causal interpretation. In this case, the causal effects of treatment on the p -th ($0 < p < 1$) quantile ([Zhang et al., 2012](#)) is defined as

$$\eta_p = q_{Y_i(1)}(p) - q_{Y_i(0)}(p), \quad (1)$$

where $q_{Y_i(t)}$ denotes the quantile associated with the distribution of potential outcome $Y_i(t)$ for $t = 0, 1$. In many applications, it is also of interest to understand the effect (on the quantiles) of applying (versus withholding) treatment among all units who are prescribed such interventions rather than the quantile effect of applying (versus withholding) treatments among all units. This

causal quantity is formally known as the quantile treatment effect on the treated and is defined as

$$\zeta_p = q_{Y_i(1)|D_i=1}(p) - q_{Y_i(0)|D_i=1}(p), \quad (2)$$

where $q_{Y_i(t)|D_i=1}$ denotes the quantile associated with the distribution of the potential outcome $Y_i(t)$ given $D_i = 1$ for $t = 0, 1$ (Zhang et al., 2012). When there exists no heterogeneity of the treatment effect by covariates (i.e., no interactions effects of treatment and confounder), the quantile treatment effect and the quantile treatment effect on the treated are identical if the effects are additive. However, when treatment heterogeneity exists, they differ (Moodie et al., 2018).

Causal effects on quantiles can be estimated using a quantile regression model with appropriate adjustment for confounders. However, it should be noted that the quantile estimates from a quantile regression model are conditional on all the covariates in the model. If one is interested in estimating the marginal quantile at a given probability level (without conditioning on covariates), it cannot be determined by a single conditional quantile alone. Zhang et al. (2012) considered the problem of estimating the causal quantities defined in (1) and (2), under parametric assumptions. Let (Y, D, \mathbf{X}) represent a generic form of the triplet (Y_i, D_i, \mathbf{X}_i) , and similarly, let $Y(t)$ denote the potential outcome of a generic unit for $i = 1, \dots, n$, $t = 0$ or 1 . The distribution of the potential outcome $Y(t)$ is given by

$$F_t(y) = E\{P(Y(t) \leq y|\mathbf{X})\} = \int G(y|t, \mathbf{x})dH(\mathbf{x}), \quad (3)$$

where $G(y|t, \mathbf{x}) = P(Y \leq y|D = t, \mathbf{X} = \mathbf{x})$, and $H(\cdot)$ denotes the marginal distribution of \mathbf{X} for $t = 0, 1$. Similarly, the conditional potential outcome $Y(t)$ given $D = 1$, is given by

$$F_{t|1}(y) = E\{P(Y(t) \leq y|\mathbf{X})|D = 1\} = \int G(y|t, \mathbf{x})dH_1(\mathbf{x}), \quad (4)$$

where $H_1(\cdot)$ denotes the marginal distribution of \mathbf{X} given $D = 1$ for $t = 0, 1$. The counterfactual distribution, given in (3), is estimated by

$$\hat{F}_t(y) = n^{-1} \sum_{i=1}^n \hat{G}(y|t, \mathbf{X}_i), \quad (5)$$

where $\hat{G}(\cdot)$ is an estimate of $G(\cdot)$ under the assumption that a normal linear model holds after a Box-Cox transformation (Zhang et al., 2012). Finally the p -th quantile $q_{Y(t)}(p)$ is estimated by inverting the estimated unconditional distribution function $\hat{F}_t(y)$ and substituting this estimate into the expression given by (1) to obtain the estimate of the quantile treatment effect for the

population. This is popularly known as outcome regression (OR) based estimate. Similarly, one can estimate $F_{t|1}(\cdot)$, given in (4), by

$$\hat{F}_{t|1}(y) = \frac{1}{\sum_{i=1}^n D_i} \sum_{i=1}^n \hat{G}(y|t, \mathbf{X}_i) D_i. \quad (6)$$

We then invert $\hat{F}_{t|1}(y)$ to obtain estimates of $q_{Y_i(t)|D_i=1}(p)$ and hence the quantile treatment effect for the treated ζ_p given in the expression (2). Alternative estimators of the counterfactual distributions proposed by Zhang et al. (2012) are based on inverse propensity weighting (IPW) and matching techniques. Firpo (2007) proposed quantile regression approach for estimation of counterfactual quantiles using inverse propensity score as weights.

3 Proposed Methodology

When the context suggests the presence of a heavy tailed nature in the data generating process and one is interested in the extreme tails of the distribution $F_t(\cdot)$ (i.e. p is close to 0 or 1), it is appropriate to model $G(\cdot)$ with some heavy tailed components. Let us denote the τ -th conditional quantile of $Y_i(t)$ as $Q_{Y_i(t)}(\tau|\mathbf{X}_i)$ at a probability level $\tau \in (0, 1)$. Then the conditional distribution of $Y_i(t)$ given \mathbf{X}_i for $i = 1, \dots, n$, can be written as (Chernozhukov et al., 2013)

$$G(y|t, \mathbf{X}_i) = \int_0^1 \mathbb{I} [Q_{Y_i(t)}(\tau|\mathbf{X}_i) \leq y] d\tau, \quad (7)$$

where $\mathbb{I}[\cdot]$ is an indicator function. A natural approximation of the conditional distribution of $Y_i(t)$ is given by

$$G(y|t, \mathbf{X}_i) = \int_0^1 \mathbb{I} [Q_{Y_i(t)}(\tau|\mathbf{X}_i) \leq y] d\tau = \sum_{j=1}^J (\tau_j - \tau_{(j-1)}) \mathbb{I} [Q_{Y_i(t)}(\tau_j|\mathbf{X}_i) \leq y], \quad (8)$$

where $\tau_1 = 0, \dots, \tau_J = 1$ are the probability levels where the quantiles are evaluated. To model the bulk and the extreme components of $G(y|t, \mathbf{X}_i)$ efficiently, we consider a suitable transition probability level $\tau_u \in (0, 1)$ and decompose (7) as follows

$$G(y|t, \mathbf{X}_i) = \int_0^{\tau_u} \mathbb{I} [Q_{Y_i(t)}(\tau|\mathbf{X}_i) \leq y] d\tau + \int_{\tau_u}^1 \mathbb{I} [Q_{Y_i(t)}(\tau|\mathbf{X}_i) \leq y] d\tau. \quad (9)$$

For a suitably chosen transition probability level τ_u , the estimate of $G(\cdot)$ is given by

$$\hat{G}(y|t, \mathbf{X}_i) = \sum_{j=1}^u (\tau_j - \tau_{(j-1)}) \mathbb{I} [\hat{Q}_{Y_i(t)}(\tau_j|\mathbf{X}_i) \leq y] + \sum_{j=u+1}^J (\tau_j - \tau_{(j-1)}) \mathbb{I} [\tilde{Q}_{Y_i(t)}(\tau_j|\mathbf{X}_i) \leq y], \quad (10)$$

where $\hat{Q}_{Y_i(t)}(\tau_j|\mathbf{X}_i)$ and $\tilde{Q}_{Y_i(t)}(\tau_j|\mathbf{X}_i)$ in the first and second summand of (10) are estimates of $Q_{Y_i(t)}(\tau_j|\mathbf{X}_i)$ based on simultaneous quantile regression and parametric extreme value modeling techniques, respectively, such that the issue of quantile crossing does not arise. The details of the proposed estimation methodology are discussed in Subsections 3.1-3.2. The estimated conditional distribution function is then plugged into (5) to obtain the counterfactual distributions $\hat{F}_t(y)$ for $t = 0, 1$. This distribution function is then inverted to estimate the quantiles $\hat{q}_{Y_i(t)}(p) = \inf\{z : \hat{F}_t(z) \geq p\}$ for $t = 0, 1$, and finally the quantile causal effect for the population η_p is given by

$$\hat{\eta}_p = \hat{q}_{Y_i(1)}(p) - \hat{q}_{Y_i(0)}(p). \quad (11)$$

Similarly, we obtain $\hat{q}_{Y_i(t)|D_i=1}(p) = \inf\{z : \hat{F}_{t|1}(z|D_i = 1) \geq p\}$ from (6), and the estimate of ζ_p is given by

$$\hat{\zeta}_p = \hat{q}_{Y_i(1)|D_i=1}(p) - \hat{q}_{Y_i(0)|D_i=1}(p).$$

3.1 Selection of Transition Point from Bulk to Extreme

The above method divides the entire probability distribution into two parts and different tools are used to estimate each of the parts. These parts are determined by the choice of the probability level τ_u in (9). The value of the τ_u th quantile determines the transition point on the distribution, below which the quantile regression model is fitted to the bulk part of the distribution of the potential outcome, and above which a heavy tailed Generalized Pareto distribution (GPD) model is fitted. Choice of the threshold and fitting of a Generalised Pareto distribution to the exceedence of the threshold is a widely studied problem in the extreme value literature. Too low and too high value of the threshold should generally be avoided (Coles, 2001). Too high a threshold leaves fewer exceedances to fit to the GPD model and may result in estimators with high variance. Too low a threshold leads to an inadequate fit to the GPD model and may result in biased estimators. In the light of the model (10), we are constrained to choose a threshold as a quantile of the conditional distribution. Many threshold selection procedures are proposed in the literature: see Scarrott and MacDonald (2012) for a review. There are broadly four categories of approaches for threshold selection. The first, and most common approach is based on a graphical diagnosis method (Davison and Smith, 1990; Drees et al., 2000; Coles, 2001).

The second approach involve methods that minimize the asymptotic mean-squared error of the estimators of the GPD parameters or of the extreme quantiles, under particular assumptions on the upper tail of the GPD (Hall, 1990; Beirlant et al., 2004; Langousis et al., 2016). The third category

of methods are based on the goodness-of-fit (gof) test of the GPD (Davison and Smith, 1990; Bader et al., 2018), where the threshold is selected at the level to ensure the GPD provides an adequate fit to the exceedances. We use the automatic threshold selection method of Bader et al. (2018) for choosing a suitable threshold. Most of the above methods can incorporate additional covariate information in different levels of the modelling. See Davison and Smith (1990) and Beirlant et al. (2005) for an extensive review of covariate dependent GPD modelling. For covariate dependent threshold selection, we use the quantile regression method proposed by Koenker (2005).

Two-step approach for selection of τ_u : To select a τ_u in (9), we develop a two-step approach. In the first step we use covariates to generate multiple competing thresholds through quantile regression (Koenker, 2005), and in the second step we adapt the automatic threshold selection method of Bader et al. (2018) to select the best threshold for controlling false discovery rate (FDR). Specifically, in the first step, for a given number l , we consider l competing thresholds as fitted quantiles $U(\tau|\mathbf{w}) = \mathbf{w}^T \hat{\boldsymbol{\alpha}}(\tau)$, where $\mathbf{v} = (D, \mathbf{X})$ and $\mathbf{w} = (1, \mathbf{v})^T$ is a covariate vector of dimension $(m + 1)$ including 1, and $\hat{\boldsymbol{\alpha}}(\tau) = (\hat{\alpha}_0(\tau), \dots, \hat{\alpha}_m(\tau))^T$ are the estimates corresponding to the regression parameter vector obtained from linear regression (Koenker, 2005) for $\tau = \tau_1, \dots, \tau_l$. Therefore, for a given set of l probability levels, the method produces thresholds $U(\tau_1|\mathbf{w}) < \dots < U(\tau_l|\mathbf{w})$.

In the second step, we adopt the approach of Bader et al. (2018) for automatically selecting a threshold from the above competing set in the presence of covariates. We use each of the thresholds, and fit a GPD to the exceedances above the threshold. A different GPD is obtained from the different covariate adjusted threshold. Then we use maximum likelihood to estimate the unknown GPD parameters. Let us assume that, for the i th threshold there are n_i exceedances, $i = 1, \dots, l$. Then the sequence of null hypotheses to be tested are $H_0^{(i)}$: the distribution of n_i observations above $U(\tau_i|\mathbf{w})$ follows the GPD.

Bader et al. (2018) improvised the ForwardStop rule of G'Sell et al. (2015) to the sequential testing (ordered) of null hypotheses H_1, \dots, H_l . The method uses the p -values corresponding to the tests of l hypotheses as $p_1, \dots, p_l \in [0, 1]$. For testing multiple hypothesis with an ordered nature, G'Sell et al. (2015) propose transforming the sequence of p -values to a monotone sequence and then applying the original method of Benjamini and Hochberg (1995) on the monotone sequence. The rejection rule is constructed by returning a cutoff \hat{k} such that $H_1, \dots, H_{\hat{k}}$ are rejected. They prescribe that if no $\hat{k} \in 1, \dots, l$ exists, then no rejection is made. ForwardStop is given by

$$\hat{k} = \max \left\{ k \in \{1, \dots, l\} : -\frac{1}{k} \sum_{i=1}^k \log(1 - p_i) \leq \lambda \right\}$$

where λ is a pre-specified level. In threshold testing, stopping at k implies that the goodness-of-fit test of the GPD to the exceedances at the first k thresholds $U(\tau_1|\mathbf{w}), \dots, U(\tau_k|\mathbf{w})$ are rejected. In other words, the set of first k null hypotheses H_1, \dots, H_k are rejected. Let us denote $U(\tau_u|\mathbf{w})$ as the GPD threshold corresponding to the selected probability level $\tau_u = \tau_{\hat{k}}$.

3.2 Estimation of Quantiles in the Bulk Part

After the selection of the transition point between the bulk and the extreme part of the distribution, the proposed method requires estimation of both parts of (9). The first part requires estimation of multiple conditional quantiles at different probability levels. One can estimate these quantiles separately and use the estimates in (8). This approach has two drawbacks. Firstly, it may be possible that multiple estimated quantiles cross each other even if their population versions never cross. For example, it may be possible that the estimated 90th percentile has a larger value than the estimated 95th percentile. This results in an invalid estimate of the corresponding distribution function. Secondly, consecutive quantiles may share common characteristic and strength (Zou and Yuan, 2008). Simultaneous estimation may improve the estimation accuracy of an individual quantile function (Liu and Wu., 2011). More recent work with associated R code is available in (Schnabel and Eilers, 2013). This work is based on using splines to model the quantile regression functions. The drawback with this method is that there is no clear theoretical justification which guarantees that there will be no crossings.

Alternatively, one can consider the method of Bondell et al. (2010) to ensure non-crossing for simultaneous quantile estimation (first part of (10)). Let $\mathbf{C} \subset \mathbb{R}^m$, be a closed convex polytope, represented as the convex hull of n points in m -dimensions. Recall that $\mathbf{v} = (D, \mathbf{X})^T$. Suppose one is interested in ensuring that the quantile curves do not cross for all values of the covariate $\mathbf{v} \in \mathbf{C}$. For estimating quantiles at probability levels $\tau_1 < \dots < \tau_u$, Bondell et al. (2010) use a simple and computationally efficient procedure to estimate non-crossing quantiles using a version of constrained optimization. The method implements a constrained version of the linear quantile regression to obtain non-crossing estimates of the conditional quantiles for all values of the covariate $\mathbf{v} \in \mathbf{C}$.

This goal is achieved by imposing appropriate dominance in every consecutive pair of quantile regression planes. Specifically, the constrained quantile regression problem becomes estimation of

regression parameters through

$$\begin{aligned}\hat{\boldsymbol{\beta}} &= \min_{\boldsymbol{\beta}} \sum_{j=1}^u \sum_{i=1}^n \rho_{\tau_j} (Y_i - \mathbf{w}_i^T \boldsymbol{\beta}(\tau_j)), \\ \text{subject to } &\mathbf{w}^T \boldsymbol{\beta}(\tau_{j+1}) \geq \mathbf{w}^T \boldsymbol{\beta}(\tau_j) \\ \text{for } &j = 1, \dots, u-1, \quad \forall \quad \mathbf{v} \in \mathbf{C},\end{aligned}\tag{12}$$

where $\rho_{\tau_j}(w) = \tau_j(1 - \mathbb{I}(w < 0))$ is the check function. Note that, the estimated conditional quantile of $Y_i(t)$ given \mathbf{X}_i in the first summand of equation (10) is given by $\hat{Q}_{Y(t)}(\tau|\mathbf{X}_i) = \hat{\beta}_0(\tau) + t\hat{\beta}_1(\tau) + \mathbf{X}_i^T \hat{\boldsymbol{\beta}}^*(\tau)$, where $\hat{\boldsymbol{\beta}}^*(\tau)$ is the $(m-1)$ dimensional estimated coefficients vector corresponding to \mathbf{X}_i , for $t = 0, 1$, $\tau = \tau_1, \dots, \tau_u$, $i = 1, \dots, n$.

3.3 Estimation of Quantiles in the Extreme Part

Suppose there exists a non-degenerate limiting distribution for appropriately linearly re-scaled exceedences of a sequence of independently and identically distributed observations Y_1, \dots, Y_n above a threshold $U(\tau_u|\mathbf{w})$. Then under general regularity conditions on max-stability, the limiting distribution will be a GPD as $U(\tau_u|\mathbf{w}) \rightarrow \infty$ (Pickands, 1975). Note that the choice of $U(\tau_u|\mathbf{w})$ provided in Subsection 3.1 guarantees the suitability of GPD to model the exceedences. The GPD is characterized by the distribution function

$$H(y|U(\tau_u|\mathbf{w}), \sigma) = \begin{cases} 1 - \left[1 + \xi \left(\frac{y - U(\tau_u|\mathbf{w})}{\sigma}\right)\right]^{-1/\xi}, & y \geq U(\tau_u|\mathbf{w}), \xi \geq 0, \\ 1 - \exp\left[\frac{y - U(\tau_u|\mathbf{w})}{\sigma}\right], & U(\tau_u|\mathbf{w}) < y < U(\tau_u|\mathbf{w}) - \sigma/\xi, \xi < 0, \end{cases}\tag{13}$$

where the threshold $U(\tau_u|\mathbf{w}) = \mathbf{w}^T \hat{\boldsymbol{\alpha}}(\tau_u)$, ξ is the shape parameter, and σ is the threshold-dependent scale parameter. The shape and scale parameters are estimated using maximum likelihood, and denoted as $\hat{\sigma}$ and $\hat{\xi}$, respectively. The estimated conditional quantile of $Y_i(t)$ at probability level $\tau = \tau_{u+1}, \dots, \tau_J$, in the second summand of equation (10) is given by the approximation (see Coles (2001), Section 4.3.3)

$$\tilde{Q}_{Y_i(t)}(\tau|\mathbf{X}_i) = \begin{cases} U^* + \frac{\hat{\sigma}}{\hat{\xi}} \left[\left(\frac{\hat{\xi}_{U^*}}{1-\tau} \right)^{\hat{\xi}} - 1 \right], & \text{if } \hat{\xi} \neq 0, \\ U^* + \hat{\sigma} \log \left(\frac{\hat{\xi}_{U^*}}{1-\tau} \right), & \text{if } \hat{\xi} = 0, \end{cases}$$

where $U^*(t, \mathbf{X}_i) = \hat{\alpha}_0(\tau_u) + t\hat{\alpha}_1(\tau_u) + \mathbf{X}_i^T \hat{\boldsymbol{\alpha}}^*(\tau_u)$ for $t = 0, 1$, and $\hat{\boldsymbol{\alpha}}^*(\tau_u)$ is the estimated regression coefficient of dimension $(m-1)$, $\hat{\xi}_{U^*} = \frac{n_{U^*}}{n}$, where n_{U^*} is the number of exceedences of the threshold

$U^*(t, \mathbf{X}_i)$ in the given sample of size n . Note that, under the assumption of a heavy tailed response distribution (with shape parameter $\xi > 0$), the above estimated quantile $\tilde{Q}_{Y_i(t)}(\tau|\mathbf{X}_i)$ is an increasing function of τ . This fact ensures no crossings for the fitted quantiles while estimating multiple probability points at extreme tails.

3.4 Bootstrap Algorithm

Zhang et al. (2012) considered the standard full sample bootstrap method to compute the standard error and confidence interval of the proposed estimators (OR, IPW, Matching, etc.) for ease of implementation, avoiding the difficulty of deriving asymptotic variance. However, the validity of the bootstrap method has not been studied. Zhang et al. (2021) considered the estimator proposed by Firpo (2007), showed that the estimator is asymptotically normal and suggested a valid full-sample bootstrap confidence interval to quantify the uncertainty. For the moderately extreme case, the paper showed that the limiting distribution of the estimator is no longer Gaussian, and proposed a b -out-of- n bootstrap for valid inference. Note that, our proposed method is different from the existing methods, and it involves steps that boil down to the problem of estimating conditional distributions (See Section 3). Recently, Litvinova and Silvapulle (2020) established the asymptotic validity of the full-sample bootstrap for constructing confidence intervals for high-quantiles, tail probabilities, and other tail parameters of a univariate distribution. Hence, we propose to employ the full sample bootstrap considering the following steps to compute the standard error and confidence interval of the proposed estimator.

- Step 1. Sample $(Y_i^*, D_i^*, \mathbf{X}_i^*)$ from the observed data (Y_i, D_i, \mathbf{X}_i) , $i = 1, \dots, n$.
- Step 2. Based on the data $(Y_i^*, D_i^*, \mathbf{X}_i^*)$, $i = 1, \dots, n$, obtain the estimates $\hat{\eta}_p^*$ and $\hat{\zeta}_p^*$.
- Step 3. Replicate Step 1 to Step 3 for N_B number of times, where N_B is a large number, say 1000.
- Step 4. Estimate the bias, standard error and confidence interval of $\hat{\eta}_p$ and $\hat{\zeta}_p$ from the N_B bootstrap estimates of $\hat{\eta}_p^*$ and $\hat{\zeta}_p^*$, respectively.

4 Simulation Study

We consider two confounding variables X_1 and X_2 , where X_1 follows a normal distribution with mean 15 and standard deviation 6, and X_2 follows an exponential distribution with mean 2. We

then consider a non-confounding variable $X_3 \sim N(1, 1)$, and specify the following relationships between the response variable Y and a binary treatment D :

$$\text{logit}[\pi(D|X_1, X_2, X_3)] = -3 + 0.1X_1 + 0.1X_2 + 0.2X_3$$

$$Y = 10 + 15D + X_1 + 3X_2 + 2X_1D + (1 + 4X_2 + 3D)\epsilon,$$

where errors ϵ are generated from two different symmetric distributions with mean 0. In the first case, we consider ϵ following a normal distribution with mean 0 and standard deviation 10 and in the second case ϵ follows a t -distribution with degrees of freedom 1. The second choice incorporates a heavy tailed component in the data. We generate data for sample sizes $n = 500$ and $n = 1000$.

The transition point representing the shift from the bulk to the extreme part (τ_u in (9)) is selected by the automated threshold selection method described in Section 3.1. As a set of competing thresholds, we use a set of 10 quantiles with equally spaced probability levels ranging from 0.75 to 0.99. We use quantile regression at each τ with covariates as treatment D , and two more predictors, X_1 , and X_2 . The fitted quantiles are then used as covariate dependent thresholds for the GPD model. The sequential multiple hypothesis approach based on Anderson-darling goodness-of-fit test of Bader et al. (2018) is then used to select the best threshold optimizing the given criteria. The selected threshold is used as the transition point and the corresponding probability level is taken as the transition probability level τ_u . We choose a total of 100 grid points in the computation of (10): 75 and 25 equidistant points for computing the first (bulk part) and the second component (extreme part), respectively. For computing the bulk part of (9), we adopt the simultaneous quantile regression approach of Bondell et al. (2010) and use the associated R package. In the extreme part of (9), we model the GPD threshold using all the covariates, and the shape and scale parameters of the GPD are estimated via maximum likelihood.

We compare the performance of the proposed estimate with the existing competitors for both population and treated, based on 1000 simulations with respect to bias, variance and mean squared error (MSE). For this purpose, we consider the targeted maximum likelihood estimate (TMLE) proposed by Díaz (2017) and the estimator proposed by Firpo (2007) along with the OR and IPW estimates proposed by Zhang et al. (2012). The results are summarized in Tables 1-4. First, we discuss the results corresponding to quantile causal effects for the population (see Tables 1-2). The relative bias (RB) associated with IPW, TMLE and Firpo estimates are very small for all the probability levels except $p = 0.995$. The RB increases significantly for all the estimates at probability level $p = 0.995$. In particular, the RB of IPW and Firpo estimates are very large

compared to the other methods at probability level $p = 0.995$ when the data generation mechanism involves a heavy tailed error distribution (see Table 2). For all the probability levels, the variance and MSE of the proposed method are smaller compared to all other methods when the data generation mechanism involves a normal error distribution (see Table 1). Similar patterns are also observed at probability level $p = 0.95$ when the data generation mechanism involves a heavy tailed error distribution (see Table 2). In this setup, the variance and MSE of all the competitive estimates are exorbitantly high compared to the proposed method at probability level $p = 0.995$. Next we consider the results corresponding to quantile causal effects for the treated (see Tables 3-4). Here, the findings are very similar to the case of causal effects on the population except for a few notable differences. The performance of all estimates except the OR method at probability level $p = 0.995$ are comparable with respect to RB when the data generation mechanism involves a normal error distribution (see Table 3). In contrast, when the data generation mechanism involves a heavy tailed error distribution, the RB of the proposed method is considerably smaller compared to all other competitive methods for $n = 500$. The variance and MSE of all the competitive estimates are considerably higher compared to the proposed method at probability level $p = 0.95$ and $p = 0.995$. This pattern is more dominant when the data generation mechanism involves a heavy tailed error distribution (see Table 4). From these observations, we can conclude that the proposed method outperforms the existing methods for estimating the causal effect at extreme quantiles.

5 Analysis of London Cycle Superhighway Effects

The main interest of this study is to evaluate the effect of CS to contain extreme congestion. If the overall traffic volume goes up but the road space is being shared with other forms of transport, then there is less space for the mobility of cars, which impacts the traffic speed on the road and therefore congestion increases (Yuan et al., 2015). The data that are available and the logic to construct the response and covariates are described below.

- (a) Annual average daily traffic (AADT): the total volume of vehicle traffic of a highway or a road for a year divided by 365 days. To measure AADT on individual road segments, traffic data is collected by an automated traffic counter, hiring an observer to record traffic or licensing estimated counts from GPS data providers. AADT is a simple but useful measurement to indicate busyness of a road.

Table 1: Quantile treatment effect at different probability levels for the population using proposed semi-parametric, OR, IPW, TMLE, and Firpo estimator based on the data generating process with Gaussian error. The relative bias (RB) is the bias relative to the true parameter value and relative variance (RV) and RMSE are relative to the variance and MSE of the proposed estimator, respectively.

p	Method	$n=500$				$n=1000$			
		Estimate	RB	RV	RMSE	Estimate	RB	RV	RMSE
0.85	OR	108.25	1.41	1.91	1.57	108.68	1.82	1.78	1.34
	IPW	106.98	0.22	1.72	1.40	107.18	0.41	1.44	1.05
	TMLE	106.46	-0.27	1.69	1.37	106.83	0.08	1.44	1.04
	Firpo	106.58	-0.16	1.70	1.38	106.99	0.23	1.43	1.04
	Proposed	101.27	-4.98	1	1	101.54	-4.72	1	1
0.90	OR	120.03	5.86	2.34	1.67	120.19	6.01	2.19	1.38
	IPW	113.43	0.05	2.46	1.54	113.80	0.38	2.03	1.01
	TMLE	112.96	-0.37	2.41	1.51	113.37	-0.01	1.01	1
	Firpo	113.12	-0.23	2.47	1.54	113.69	0.28	2.03	1.01
	Proposed	106.11	-12.40	1	1	104.29	-7.85	1	1
0.95	OR	137.67	13.76	3.46	2.17	137.30	13.46	3.24	1.83
	IPW	121.52	0.42	4.86	1.97	121.86	0.70	4.29	1.24
	TMLE	121.22	0.17	4.61	1.87	121.29	0.23	4.16	1.20
	Firpo	120.94	-0.06	4.97	2.02	121.62	0.50	4.39	1.27
	Proposed	106.12	-12.18	1	1	106.27	-12.04	1	1
0.995	OR	184.00	33.02	10.15	3.28	181.53	31.23	9.58	2.62
	IPW	124.89	-9.65	67.99	9.62	136.05	-1.64	62.55	5.49
	TMLE	162.98	17.82	26.16	4.18	173.56	25.47	25.69	3.44
	Firpo	128.10	-7.39	85.20	11.95	131.89	-4.65	69.13	6.10
	Proposed	107.26	-22.43	1	1	107.39	-22.33	1	1

Table 2: Quantile treatment effect at different probability levels for the population using proposed semi-parametric, OR, IPW, TMLE, and Firpo estimator based on the data generating process with heavy tailed error from t-distribution. The relative bias (RB) is the bias relative to the true parameter value and relative variance (RV) and RMSE are relative to the variance and MSE of the proposed estimator, respectively.

p	Method	$n=500$				$n=1000$			
		Estimate	RB	RV	RMSE	Estimate	RB	RV	RMSE
0.85	OR	110.09	34.47	9339.33	2287.53	97.99	19.70	20828.91	3082.84
	IPW	81.95	0.10	0.23	0.06	81.87	0.01	0.20	0.03
	TMLE	81.67	-0.24	0.58	0.58	81.68	-0.23	0.20	0.03
	Firpo	81.81	-0.07	0.58	0.58	81.78	-0.10	0.20	0.03
	Proposed	101.27	23.75	1	1	101.54	24.09	1	1
0.90	OR	123.86	43.75	13059.20	3889.35	108.78	26.24	28468.27	5438.10
	IPW	86.75	0.67	0.51	0.15	86.32	0.18	0.42	0.08
	TMLE	87.67	1.74	2.15	0.64	84.81	-1.58	3.89	0.74
	Firpo	86.55	0.44	0.51	0.15	86.20	0.04	0.42	0.08
	Proposed	104.12	-12.40	1	1	104.29	21.06	1	1
0.95	OR	144.97	54.49	20206.96	9903.67	124.95	33.15	43483.93	15341.32
	IPW	98.54	5.01	6.40	3.21	96.43	2.75	4.08	1.47
	TMLE	102.01	8.70	64.21	31.66	92.73	-1.19	98.15	34.62
	Firpo	97.88	4.31	6.32	3.15	96.10	2.40	3.82	1.37
	Proposed	106.12	13.26	1	1	106.27	13.42	1	1
0.995	OR	204.63	-35.02	47624.65	171.74	168.87	-46.38	103300.70	220.34
	IPW	1170.64	271.71	404897.20	1474.67	1353.69	329.83	2193302	4692.91
	TMLE	622.46	97.65	199931.40	721.93	217.14	-31.05	172301.40	366.89
	Firpo	1850.45	487.56	1643411.01	5971.25	666.34	111.58	64430.41	139.99
	Proposed	107.26	-65.92	1	1	107.39	-65.87	1	1

Table 3: Quantile treatment effect at different probability levels for the treated using proposed semi-parametric, OR, IPW, TMLE, and Firpo estimator based on the data generating process with Gaussian error. The relative bias (RB) is the bias relative to the true parameter value and relative variance (RV) and RMSE are relative to the variance and MSE of the proposed estimator, respectively.

p	Method	$n=500$				$n=1000$			
		Estimate	RB	RV	RMSE	Estimate	RB	RV	RMSE
0.85	OR	98.48	-13.28	2.19	1.95	98.74	-13.05	1.05	1.68
	IPW	111.37	-1.93	2.20	1.05	112.96	-0.53	1.95	0.59
	TMLE	111.76	-1.59	2.09	1	113.01	-0.47	1.90	0.58
	Firpo	111.52	-1.79	2.20	1.05	113.03	-0.52	1.95	0.59
	Proposed	104.81	-10.12	1	1	101.26	-10.60	1	1
0.90	OR	110.70	-7.50	3.03	1.38	111.43	-6.90	2.83	0.88
	IPW	116.47	-2.69	3.32	1.28	118.69	-0.83	2.96	0.69
	TMLE	111.58	-2.59	3.29	1.27	118.65	-0.86	2.99	0.70
	Firpo	116.61	-2.57	3.32	1.28	118.79	-0.74	2.97	0.69
	Proposed	104.70	-12.25	1	1	103.99	-12.85	1	1
0.95	OR	136.75	7.97	5.83	1.76	137.83	8.82	5.54	1.34
	IPW	120.98	-4.49	9.39	2.58	124.87	-1.41	7.21	1.16
	TMLE	120.96	-4.50	7.75	2.14	124.74	-1.52	7.43	1.19
	Firpo	121.12	-4.38	9.43	2.59	125.00	-1.31	7.20	1.15
	Proposed	106.71	-15.52	1	1	106.01	-16.10	1	1
0.995	OR	230.87	61.36	38.84	9.58	246.86	72.53	49.56	10.73
	IPW	105.48	-26.28	97.70	11.31	111.81	-21.86	124.81	8.20
	TMLE	108.63	-24.87	88.88	10.22	113.99	-20.33	112.53	7.37
	Firpo	106.41	-25.63	102.87	11.80	111.87	-21.81	132.73	8.68
	Proposed	107.88	-24.78	1	1	107.26	-25.21	1	1

Table 4: Quantile treatment effect at different probability levels for the treated using proposed semi-parametric, OR, IPW, TMLE, and Firpo estimator based on the data generating process with heavy tailed error from t-distribution. The relative bias (RB) is the bias relative to the true parameter value and relative variance (RV) and RMSE are relative to the variance and MSE of the proposed estimator, respectively.

p	Method	$n=500$				$n=1000$			
		Estimate	RB	RV	RMSE	Estimate	RB	RV	RMSE
0.85	OR	-99.24	-212.73	9675.98	3670.50	-164.15	-286.46	12408.78	3583.60
	IPW	87.33	-0.80	0.95	0.33	87.55	-0.55	0.27	0.07
	TMLE	87.40	-0.72	0.88	0.31	87.60	-0.50	0.25	0.07
	Firpo	87.38	-0.75	0.95	0.33	87.57	-0.52	0.27	0.07
	Proposed	78.92	-10.30	1	1	101.55	15.41	1	1
0.90	OR	-137.39	-249.68	11638.38	4077.37	-216.18	-335.51	16327.94	5808.879
	IPW	90.44	-1.47	2.20	0.72	91.25	-0.59	0.61	0.20
	TMLE	90.63	-1.26	1.65	0.54	91.29	-0.54	0.55	0.18
	Firpo	90.48	-1.43	2.20	0.72	91.28	-0.56	0.61	0.20
	Proposed	80.88	-11.86	1	1	104.29	13.70	1	1
0.95	OR	-182.95	-284.48	17215.69	3351.80	-283.42	-385.79	23992.99	9214.41
	IPW	97.46	-1.72	12.35	2.24	98.48	-0.71	3.47	1.25
	TMLE	97.38	-1.81	11.98	2.18	98.47	-0.71	3.27	1.25
	Firpo	97.62	-1.56	12.43	2.26	98.52	-0.66	3.48	1.25
	Proposed	82.24	-16.96	1	1	106.27	7.44	1	1
0.995	OR	897.19	181.86	684446.40	762.09	28.01	-91.20	60045.92	121.79
	IPW	699.81	119.86	687796.50	762.50	-39.91	-112.54	394287.10	790.43
	TMLE	916.50	187.93	654062.50	728.92	278.05	-12.65	6913.46	13.85
	Firpo	685.04	115.22	778969.20	863.04	175.27	-44.94	19493.28	39.39
	Proposed	82.52	-74.41	1	1	107.39	-66.59	1	1

- (b) Total Cycle Collisions (TCS): total number of cycle collisions causing injury based on police records from the STATS19 accident reporting form and collected by the UK Department for Transport. The location of an accident is recorded using coordinates which are in accordance with the British National Grid coordinate system. The CS routes were intended to reduce the risk of accidents for cyclists and the route allocation is possibly influenced by TCS. It is expected that the accident rates will affect the traffic characteristics.
- (c) Bus-stop density: the ratio of the number of bus-stops to the road length. The presence of bus-stops is expected to affect the traffic flow and speed due to frequent bus-stops and pedestrian activities. The allocation of CS routes were designed to avoid areas with high bus-stop density for safety of the cyclists.
- (d) Road network density: with the available geographical information system we could also represent the road network density in each zone by using a measure of the number of network nodes per unit of area. A network node is defined as the meeting point of two or more links. To safeguard from conflicting turning movements the CS paths are routed through the areas with high road network density.
- (e) Road length: high capacity networks tend to depress land values which in turn will influence the socio-economic profile of the people who live close together. Data for road length for each zone was generated using geographical information system software.
- (f) Road type: a binary variable where '1' represents dual-carriageway and '0' represents single-carriage. This is an important feature since we might expect traffic congestion in single-carriage roads.
- (g) Density of domestic buildings: this is a potentially useful feature since we might expect congestion to be associated with the nature of land use and the degree of urbanization. Also, the allocation of the CS paths are possibly influenced by land use characteristics.
- (h) Density of non-domestic buildings: rising housing costs in business and office districts force people to live further away, lengthening commutes, and affecting traffic flow and speed. As mentioned before, this feature may influence allocation of the CS paths.
- (i) Road area density: the ratio of the area of the zone's total road network to the land area of the zone. The road network includes all roads in the including motorways, highways, main or

national roads, secondary or regional roads. It is expected that the traffic flow is associated with road density.

- (j) Employment density: traffic generation potential depends on economic activity and we proxy this by employment density. High employment density tends to influence pedestrian activity which in turn affects traffic speed. The CS paths are designed to provide coverage in the areas with high employment density and encourage commuters to use cycling as a regular mode of transport.

Figure 3 shows density plot of AADT, exhibiting heavy tailed nature of the response variable. Using

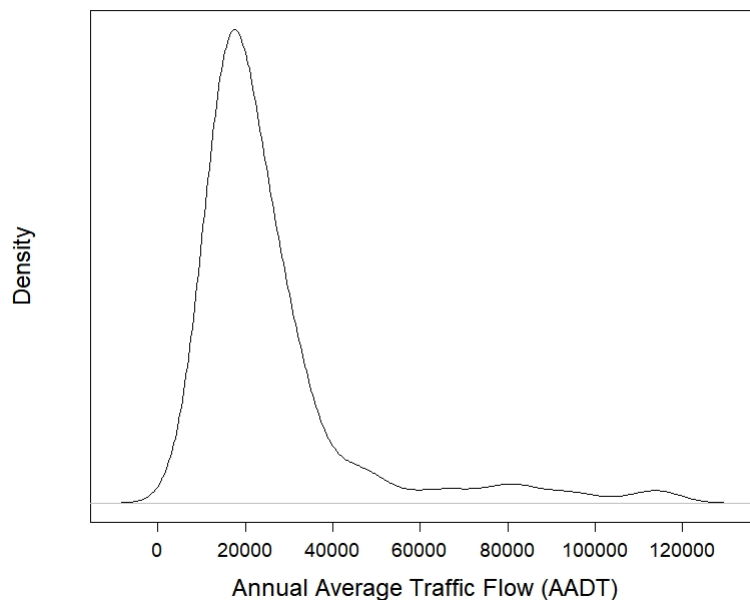


Figure 3: Density of traffic flow in London metropolitan area.

the proposed method we estimate the quantile treatment effects for the population and for the treated at different intermediate and extreme quantiles corresponding to probability levels $p=0.085$, 0.90 , 0.95 and 0.995 . As the performance of the TMLE is similar to IPW and Firpo estimates in simulation study, we only consider the OR, IPW and Firpo methods along with the proposed method for our analysis. The propensity model include the following factors: total cycle collision, bus-stop density, road network density, road length, density of domestic buildings, density of non-domestic buildings, road area density, and employment density. The OR and proposed method

consider density of domestic buildings, density of non-domestic buildings, road area density, road network density, road type, bus-stop density as covariates. The estimated quantile treatment effects of CS on annual average daily traffic (AADT) relative to the respective quantile of AADT in the pre-intervention period are presented in Table 5-6. The standard errors (SE) and the corresponding 95% confidence intervals (CI) for all the estimates, with the exception of Firpo estimate at probability level $p = 0.995$, are obtained from 1000 full bootstrap samples. To find the SE and CI of the causal effects based on Firpo method at probability level $p = 0.995$, we employ b -out-of- n bootstrap proposed by Zhang et al. (2021). See Section 3.4 for details.

The result based on the proposed estimate indicate roughly 29% increase in traffic flow compared to the pre-intervention period at probability levels $p = 0.995$ both for the entire city and the treated locations. The 95% bootstrap CI for the proposed estimate exclude 0, suggesting a significant effect of CS on AADT. However, as observed in the simulation study, the SE of the estimated causal effects of CS at probability level $p = 0.995$ based on OR, IPW and Firpo methods are very high and the most of the results are not significant. The SE of the proposed method is significantly lower than those of the OR, IPW and Firpo methods which is also reflected in the width of the confidence intervals at all probability levels for treated. A similar pattern is also observed for the population estimates at probability levels $p = 0.95$ and 0.995 .

Overall, our analysis indicates that the introduction of CS can trigger extreme traffic flows. The protected cycleways in London including CS is just over 1% of the capital's roads and CS is only a quarter of the protected cycleways. In 2020, the five busiest roads in the U.K. were in London, however, none of these five roads is within proximity of cycleways. It is important to note that such findings only reflect an average scenario rather than the extreme cases. The U.K. has 38.3 million registered motor vehicles, up from 27 million in 2007. With cities such as London not appreciably adding road capacity with a massive expansion of motor vehicles will lead to traffic congestion (Reid, 2021). The results from our analysis are insightful, but for a comprehensive understanding to formulate effective transport strategies, the effect of the cycleways on speed requires further investigation. It is important that state of the art methods are applied in such important applications and given the superiority of our methods over existing competitors provide a framework for analysis of high consequence events.

Table 5: Effect of CS on AADT relative to the respective quantile of AADT in the pre-intervention period for population.

p	Method	Estimate (%)	SE	95% CI
0.85	OR	43.34	11.50	(25.36, 70.85)
	IPW	51.41	73.06	(-3.27, 219.09)
	Firpo	108.17	22.37	(41.85, 135.01)
	Proposed	98.52	19.76	(65.19, 135.09)
0.90	OR	41.33	11.18	(22.88, 65.65)
	IPW	128.95	51.70	(0.35, 101.92)
	Firpo	121.26	15.39	(30.40, 97.85)
	Proposed	71.60	14.40	(47.07, 97.63)
0.95	OR	37.60	10.43	(19.07, 59.49)
	IPW	61.50	19.66	(0.31, 83.81)
	Firpo	59.69	9.71	(19.21, 61.45)
	Proposed	44.98	8.91	(28.57, 60.86)
0.995	OR	36.71	20.81	(-9.16, 69.66)
	IPW	2.08	9.32	(-4.78, 22.92)
	Firpo	-0.95	15.88	(-19.21, 40.90)
	Proposed	29.11	5.86	(19.31, 39.77)

Table 6: Effect of CS on AADT relative to the respective quantile of AADT in the pre-intervention period for treated.

p	Method	Estimate (%)	SE	95% CI
0.85	OR	41.27	15.90	(14.56, 71.44)
	IPW	49.69	17.10	(21.55, 81.00)
	Firpo	50.80	23.11	(26.97, 99.01)
	Proposed	44.65	8.76	(30.56, 62.12)
0.90	OR	50.27	10.09	(21.61, 62.42)
	IPW	60.94	13.51	(19.69, 71.28)
	Firpo	67.85	19.45	(18.78, 82.99)
	Proposed	37.71	7.27	(25.95, 52.19)
0.95	OR	45.04	8.65	(26.46, 59.49)
	IPW	38.19	13.46	(14.21, 69.27)
	Firpo	71.63	17.82	(20.72, 76.37)
	Proposed	34.31	7.04	(23.06, 48.46)
0.995	OR	-8.51	25.50	(-80.79, 21.02)
	IPW	15.53	8.79	(-2.37, 26.51)
	Firpo	17.48	15.62	(3.08, 63.71)
	Proposed	28.80	5.90	(19.27, 40.13)

6 Discussions

In this article we have introduced a methodology that can be used to derive inference for causal effects on extreme quantiles. We have modelled the relationships between the covariates and the response and use those relationships to predict both the treatment statuses and estimate the treatment effect at certain extreme quantiles. The key methodological insight is that improvising the conventional OR model to combine a semiparametric quantile regression framework with a heavy tailed GPD component for extreme tail, addressed issues with model misspecification due to parametric assumptions and accounts for the high variability at the extreme tails of the distribution. The inverse propensity weighted (IPW) estimate of [Zhang et al. \(2012\)](#) and the estimator proposed by [Firpo \(2007\)](#) are attractive alternative for estimating causal effects for heavy tailed distributions at intermediate quantiles to avoid some of the parametric assumptions associated with the form of the regression and/or link function which is essential in the OR approach. But these estimators exhibit high volatility at the extreme tails similar to that of the OR method, whereas our method performs significantly better than all the existing competitors.

In observational studies, one can never be sure that a model for the treatment assignment mechanism or an outcome regression model are correct. An alternative approach is to develop a doubly-robust (DR) estimator. Several DR estimation methodologies are proposed in the literature ([Kang and Schafer, 2007](#)). The approach suggested by [Zhang et al. \(2012\)](#) for doubly robust estimation for quantile causal effects is not readily extendable to our case. However, one can use augmented regression methods considering a suitable function of the propensity score $\phi(\pi(D_i|x_i, \hat{\gamma}))$ as an additional covariate in (12) and (13). Although empirical validation of the DR property seems possible, the study of theoretical properties is a challenging problem under the current set-up. One can further develop a new doubly robust estimation methodology based on the targeted maximum likelihood approach considered by [Díaz \(2017\)](#).

We have used the proposed method to analyse the effect of London Cycle Superhighways. Our results suggest that the introduction of Cycle Superhighways can increase traffic flow in the extremes, encouraging further research and a cautious approach for any possible extension of Cycle Superhighways in metropolitan cities like London, which are heavily affected by congestion. Also, it is of great interest for general public and epidemiologists, particularly in light of the increase in cycling and the recent proliferation of emergency cycle lanes to support safe community during the pandemic. Despite these interventions, we are also seeing more commuting by private vehicles as

people are trying to avoid public transport (Reid, 2021), hence an understanding of impact on cycle lanes on congestion is vital.

It is also worth noting that we are obliged to assume that the outcomes of one unit are not affected by the treatment assignment of any other units. While not always plausible, we attempt to reduce the “spillover” effects by reducing interactions between the treated and control units. One possible direction of further studies could be using an improved design and defining several types of treatment effects following Hudgens and Halloran (2008) and Barkley et al. (2020), and develop associated estimation methodologies for the setting where there may be clustered interference. Assessment of competing estimators of quantile effects at extreme tails which lies beyond the range of sample data could be another direction of future research. The data driven method for assessment of marginal extreme quantile estimates of Gandy et al. (2021) can be extended in the presence of covariates to assess the quantile estimates and thus could be used to assess causal effects at extreme quantiles.

Acknowledgement

The authors would like to acknowledge the Lloyd’s Register Foundation for funding this research through the programme on Data-Centric Engineering at the Alan Turing Institute. The authors are also grateful to Dr. Haojie Li for providing the London Traffic data set, and Professor Almut Veraart for many helpful comments and suggestions.

References

- Bader, B., Yan, J., and Zhang, X. (2018). Automated threshold selection for extreme value analysis via ordered goodness-of-fit tests with adjustment for false discovery rate. *Ann. Appl. Stat.*, 12(1):310–329. 11, 15
- Badoe, D. A. and Miller, E. J. (2000). Transportation-land-use interaction: empirical findings in north america, and their implications for modeling. *Transportation Research Part D: Transport and Environment*, 5(4):235–263. 6
- Barkley, B. G., Hudgens, M. G., Clemens, J. D., Ali, M., and Emch, E. E. (2020). Causal inference from observational studies with clustered interference, with application to a cholera vaccine study. *Annals of Applied Statistics*, 14(3):1432–1448. 27

- Beirlant, J., Goegebeur, Y., Segers, J., Teugels, J., De Waal, D., and Ferro, C. (2004). *Statistics of Extremes: Theory and Applications*. Wiley Series in Probability and Statistics. John Wiley & Sons. 10
- Beirlant, J., Goegebeur, Y., Teugels, J., and Segers, J. (2005). *Statistics of Extremes*. Wiley-Blackwell, 1 edition. 11
- Benjamini, Y. and Hochberg, Y. (1995). Controlling the false discovery rate: A practical and powerful approach to multiple testing. *Journal of the Royal Statistical Society. Series B (Methodological)*, 57(1):289–300. 11
- Blunden, M. (2016). Cycle superhighways make traffic worse in the city, report reveals. *Evening Standard*, Oct 5. 3
- Bondell, H. D., Reich, B. J., and Wang, H. (2010). Noncrossing quantile regression curve estimation. *Biometrika*, 97(4):825–838. 12, 15
- Chen, C., Jia, Z., and Varaiya, P. (2001). Causes and cures of highway congestion. *IEEE Control Systems Magazine*, 21(6):26–32. 6
- Chernozhukov, V., Fernández-Val, I., and Melly, B. (2013). Inference on counterfactual distributions. *Econometrica*, 81(6):2205–2268. 4, 9
- Coles, S. G. (2001). *An Introduction to Statistical Modeling of Extreme Values*. Springer, London. 5, 10, 13
- Davison, A. C. and Smith, R. L. (1990). Models for exceedances over high thresholds. *Journal of the Royal Statistical Society. Series B (Methodological)*, 52(3):393–442. 10, 11
- Drees, H., de Haan, L., and Resnick, S. (2000). How to make a hill plot. *Ann. Statist.*, 28(1):254–274. 10
- Díaz, I. (2017). Efficient estimation of quantiles in missing data models. *Journal of Statistical Planning and Inference*, 190:39–51. 4, 6, 7, 15, 26
- Embrechts, P., Klüppelberg, C., and Mikosch, T. (1997). *Modelling Extremal Events*. Berlin: Springer. 5

- Engelke, S. (2020). Graphical models and causality for extreme events. [5](#)
- FarahaCarlos, H. and Azevedo, L. (2017). Safety analysis of passing maneuvers using extreme value theory. *IATSS Research*, 41:12–21. [6](#)
- Firpo, S. (2007). Efficient semiparametric estimation of quantile treatment effects. *Econometrica*, 75:259–276. [4](#), [5](#), [9](#), [14](#), [15](#), [26](#)
- Fisher, R. A. and Tippett, L. H. C. (1928). Limiting forms of the frequency distribution of the largest or smallest member of a sample. *Mathematical Proceedings of the Cambridge Philosophical Society*, 24(2):180–190. [5](#)
- Freedman, D. A. (2010). *Statistical Models and Causal Inference: A Dialogue with the Social Sciences*. Cambridge University Press. [3](#)
- Frölich, M. and Melly, B. (2013). Unconditional quantile treatment effects under endogeneity. *Journal of Business & Economic Statistics*, 31:346–357. [4](#)
- Gandy, A., Jana, K., and Veraart, A. E. D. (2021). Scoring predictions at extreme quantiles. *Journal of the Royal Statistical Society. Series B (Methodological)*. [27](#)
- Gangl, M. (2010). Causal inference in sociological research. *Annual Review of Sociology*, 36:21–47. [3](#)
- Gissibl, N. and Klüppelberg, C. (2018). Max-linear models on directed acyclic graphs. *Bernoulli*, 24(4A):2693–2720. [5](#)
- Gissibl, N., Klüppelberg, C., and Otto, M. (2017). Tail dependence of recursive max-linear models with regularly varying noise variables. *arXiv: 1701.07351*. [5](#)
- Gnecco, N., Meinshausen, N., Peters, J., and Engelke, S. (2019). Causal discovery in heavy-tailed models. *arXiv: 1908.05097*. [5](#)
- G’Sell, M. G., Wager, S., Chouldechova, A., and Tibshirani, R. (2015). Sequential selection procedures and false discovery rate control. *Journal of the Royal Statistical Society: Series B (Statistical Methodology)*, 78(2):423–444. [11](#)

- Hall, P. (1990). Using the bootstrap to estimate mean squared error and select smoothing parameter in nonparametric problems. *Journal of Multivariate Analysis*, 32(2):177 – 203. 10
- Hannart, A. and Naveau, P. (2018). Probabilities of causation of climate changes. *Journal of Climate*, 31(14):5507–5524. 5
- Hudgens, M. G. and Halloran, M. E. (2008). Toward causal inference with interference. *Journal of the American Statistical Association*, 103(482):832–842. 27
- Imbens, G. W. and Rubin, D. B. (2015). *Causal inference in statistics, social, and biomedical sciences*. Cambridge University Press. 3
- Jin, J. and Rafferty, P. (2017). Does congestion negatively affect income growth and employment growth? empirical evidence from us metropolitan regions. *Transport Policy*, 55:1–8. 2
- Kang, J. D. Y. and Schafer, J. L. (2007). Demystifying double robustness: A comparison of alternative strategies for estimating a population mean from incomplete data. *Statistical*, 22(4):523–539. 26
- Koenker, R. (2005). *Quantile regression*. Cambridge University press. 11
- Langousis, A., Mamalakis, A., Puliga, M., and Deidda, R. (2016). Threshold detection for the generalized pareto distribution: Review of representative methods and application to the noaa ncdc daily rainfall database. *Water Resources Research*, 52(4):2659–2681. 10
- Li, H., J., G. D., and Liu, P. (2017). Safety effects of the london cycle superhighways on cycle collisions. *Accident Analysis and Prevention*, 99:90–101. 3, 6
- Litvinova, S. and Silvapulle, M. J. (2020). Consistency of full-sample bootstrap for estimating high-quantile, tail probability, and tail index. *arXiv:2004.12639*. 14
- Liu, Y. and Wu., Y. (2011). Simultaneous multiple non-crossing quantile regression estimation using kernel constraints. *Journal of nonparametric statistics*, 23(2):415–437. 12
- Melly, B. (2006). Estimation of counterfactual distributions using quantile regression. *Rev. Labor Econ.*, 68:543–572. 4

- Mhalla, L., Chavez-Demoulin, V., and Dupuis, D. J. (2019). Causal mechanism of extreme river discharges in the upper danube basin network. [5](#)
- Moodie, E. E. M., Saarela, O., and Stephens, D. A. (2018). A doubly robust weighting estimator of the average treatment effect on the treated. *Stat*, 7(1). [8](#)
- Naveau, P., Hannart, A., and Ribes, A. (2020). Statistical methods for extreme event attribution in climate science. *Annual Review of Statistics and Its Application*, 7(1):null. [5](#)
- Norman, W. (2017). Bike lanes don’t clog up our roads, they keep london moving. *The Gaurdian*, Dec 1. [3](#)
- Pickands, J. (1975). Statistical inference using extreme order statistics. *Ann. Statist.*, 3(1):119–131. [13](#)
- Reid, C. (2021). None of top five congested roads in u.k. feature adjacent cycleways. *Forbes*, Dec 7. [2](#), [23](#), [27](#)
- Retallack, A. and Ostendorf, B. (2019). Current understanding of the effects of congestion on traffic accidents. *Int J Environ Res Public Health*, 13(16(18)). [2](#)
- Ribes, A., Thao, S., and Cattiaux, J. (2020). Describing the relationship between a weather event and climate change: a new statistical approach. *Journal of Climate*, 0(0):null. [5](#)
- Rosenbaum, P. and Rubin, D. B. (1983). The central role of the propensity score in observational studies for causal effec. *Biometrika*, 40:41–55. [7](#)
- Scarrott, C. and MacDonald, A. (2012). Review of extreme value threshold estimation and uncertainty quantification. *REVSTAT*, 10(1). [10](#)
- Schnabel, S. K. and Eilers, P. H. C. (2013). Simultaneous estimation of quantile curves using quantile sheets. *AStA Advances in Statistical Analysis*, 97:77–87. [12](#)
- Slawson, N. (2017). Traffic jams on major uk roads cost economy around £9bn. *The Gaurdian*, Oct 18. [2](#)
- Transport for London (2010). Cycling revolution london. [2](#)
- Transport for London (2011). Barclays cycle superhighways evaluation of pilot routes 3 and 7. [3](#)

- UN Environment Programme (2019). Cycling, the better mode of transport. <https://www.unep.org/news-and-stories/story/cycling-better-mode-transport>, June 11. 2
- United Nations (2021). World bicycle day. <https://www.un.org/en/observances/bicycle-day>, June 03. 2
- Xian, X., Ye, H., Wang, X., and Lie, K. (2021). Spatiotemporal modeling and real-time prediction of origin-destination traffic demand. *63*, 1(77-89). 2
- Xu, D., Daniels, M. J., and Winterstein, A. G. (2018). A bayesian nonparametric approach to causal inference on quantiles. *Biometrics*, 74:259–276. 4
- Xu, L. and Nusholtz, G. (2017). Application of extreme value theory to crash data analysis. *The Stapp Car Crash Journal*, 61:287–298. 6
- Yuan, K., Knoop, V. L., and Hoogendoorn, S. P. (2015). Capacity drop: Relationship between speed in congestion and the queue discharge rate. *Transportation Research Record*, 2491(1):72–80. 16
- Zhang, K., Sun, D. J., Shen, S., and Zhu, Y. (2017). Analyzing spatiotemporal congestion pattern on urban roads based on taxi gps data. *Journal of Transport and Land Use*, 10(1):675–694. 6
- Zhang, N., J., G. D., Hörcher, D., and Bansal, P. (2021). A causal inference approach to measure the vulnerability of urban metro systems. *Transportation*. 3, 14, 23
- Zhang, Y. (2018). Extremal quantile treatment effects. *The Annals of Statistics*, 46(6B):3707 – 3740. 5
- Zhang, Z., Chen, Z., Troendle, J. F., and Zhang, J. (2012). Causal inference on quantiles with an obstetric application. *Biometrics*, 68(3):697–706. 4, 7, 8, 9, 14, 15, 26
- Zheng, L. and Sayed, T. (2019). Application of extreme value theory for before-after road safety analysis. *Transportation Research Record: Journal of the Transportation Research Board*, 2673. 6
- Zou, H. and Yuan, M. (2008). Regularized simultaneous model selection in multiple quantiles regression. *Computational Statistics & Data Analysis*, 52(12):5296 – 5304. 12